Supporting Information

The role of Cr^{3+} and Cr^{4+} in emission brightness enhancement and sensitivity improvements of NIR-emitting Nd^{3+}/Er^{3+} ratiometric luminescence thermometers

W. Piotrowski[1], L. Dalipi[2], R. Szukiewicz[3], B. Fond[2], M. Dramicanin[4], L. Marciniak[1]*

[1]Institute of Low Temperature and Structure Research, Polish Academy of Sciences, Okólna 2, 50-422 Wroclaw, Poland

[2] Institute of Fluid Dynamics and Thermodynamics, Otto-von-Guericke University Magdeburg, 39106 Magdeburg, Germany

[3] Institute of Experimental Physics, Faculty of Physics and Astronomy, University of Wroclaw, Wroclaw 50-204, Poland

[4]Vinča Institute of Nuclear Sciences - National Institute of the Republic of Serbia, University of Belgrade, P.O. Box 522, Belgrade 11001, Serbia.

* corresponding author: l.marciniak@intibs.pl

KEYWORDS luminescent thermometry, triple-doped nanocrystals, sensitization by transition metals, host-sensitizer-emitter systems, lanthanide ions

The integral intensities of the Nd^{3+} and Er^{3+} bands to calculate LIR values were fitted with Mott-Seitz equation (Eq. S1):

$$I = \frac{I_0}{C \cdot \exp(-\frac{W}{k \cdot T}) + 1} \quad \text{(Eq. S1)}$$

where: I – the intensity in temperature T, I_0 – the intensity in the initial temperature, W - the activation energy, k – Boltzmann constant, C – the dimensionless constant

The average lifetime of the excited states were calculated with the equation Eq. S2:

$$\langle \tau \rangle = \frac{A_1 \tau_1^{\,2} + A_2 \tau_2^{\,2}}{A_1 \tau_1 + A_2 \tau_2} \quad \text{(Eq. S2a)}$$

where: τ_1, τ_2 – the average time, which is in accordance with the relation $\tau = t \cdot \ln(2)$ and A_1, A_2 – amplitude, which are the parameters of the doubleexponential function:

$$y = y_0 + A_1 \cdot \exp(-\frac{x}{t_1}) + A_2 \cdot \exp(-\frac{x}{t_2}) \quad \text{(Eq. S2b)}$$

Temperature determination uncertainty was calculated using Eq. S6:

$$\delta T = \frac{1}{S_R} \cdot \frac{\delta LIR}{LIR} \quad \text{(Eq. S3a)}$$

S_R is the relative sensitivity and δLIR/LIR determines the uncertainty of the LIR determination, where δLIR/LIR was determined as follows:

$$\frac{\delta LIR}{LIR} = \sqrt{\left(\frac{\delta I_{Tb}}{I_{Tb}}\right)^2 + \left(\frac{\delta I_{Eu}}{I_{Eu}}\right)^2} \quad \text{(Eq. S3b)}$$

Table S1. The Rietveld refinement parameters of XRD patterns for YAG:Nd^{3+}, Er^{3+}, $Cr^{3+/4+}$ powders

Sample	Rexp	Rprofile	weigth R profile	D statisctics	weight S-Statistics
YAG:1%Nd^{3+}, 1%Er^{3+}	1.52919	1.96616	3.1929	1.33710	1.07269
YAG:1%Nd^{3+}, 1%Er^{3+}, 1%Cr^{3+}	1.55303	3.36102	4.73781	0.40631	0.25277
YAG:1%Nd^{3+}, 1%Er^{3+}, 2%Cr^{3+}	1.53677	2.51937	3.52202	0.70730	0.49693
YAG:1%Nd^{3+}, 1%Er^{3+}, 5%Cr^{3+}	1.52759	2.66131	3.75056	0.57502	0.39426
YAG:1%Nd^{3+}, 1%Er^{3+}, 10%Cr^{3+}	1.55828	1.66312	2.39261	0.81267	0.73250

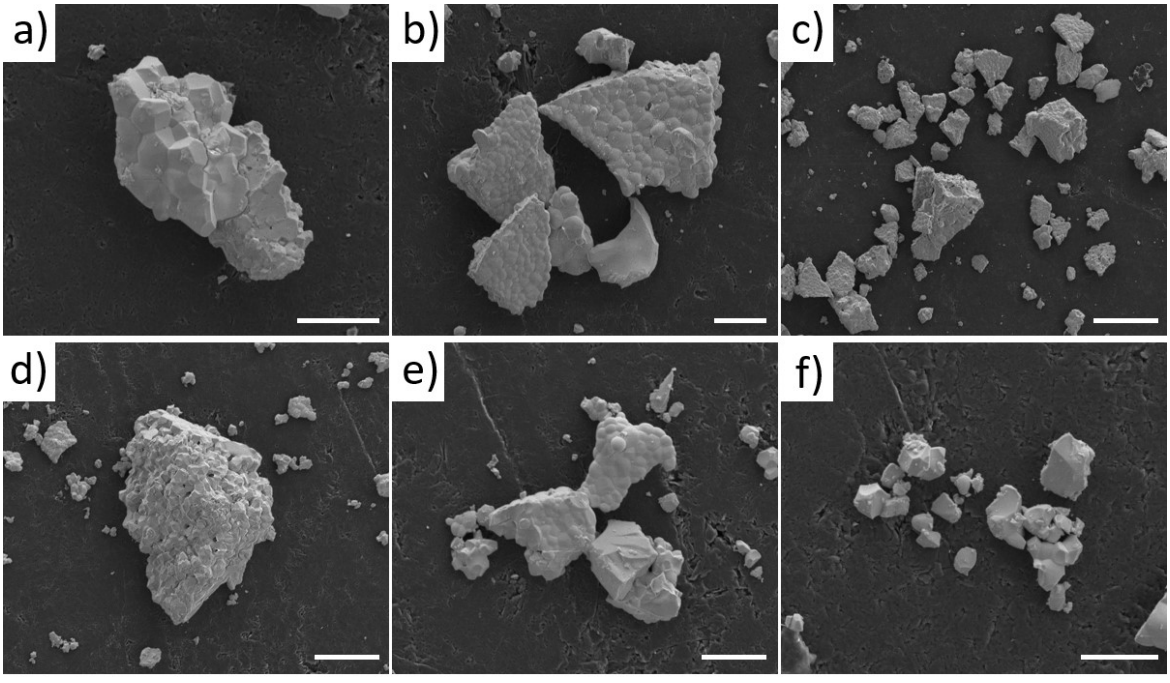

Figure S1. The representative SEM images of YAG:Nd^{3+}, Er^{3+} – scale bar: 4 μm (a), 5 μm (b), 20 μm (c) and YAG:Nd^{3+}, Er^{3+}, 10% $Cr^{3+/4+}$ – scale bar: 10 μm (d), 5 μm (e), 3 μm (f).

YAG:1%Nd^{3+}, 1%Er^{3+}, 20%Cr^{3+}	1.56894	1.82007	2.74488	0.78064	0.69035

Table S2. Atomic concentration of the surface of the analysed samples by EDS method.

	YAG:1% Nd^{3+}, 1%Er^{3+}, $Cr^{3+/4+}$-unco-doped			doped with 10% $Cr^{3+/4+}$		
Element	at% (%)	+/-	r_{conc} (%)	at% (%)	+/-	r_{conc} (%)
Y	13.630	0.166		14.097	0.284	
Nd	0.180	0.022	1.321	0.187	0.045	1.324
Er	0.163	0.012	1.198	0.180	0.008	1.277
Al	25.877	0.337		24.773	0.198	
Cr	-	-		1.947	0.123	7.858
O	60.147	0.373		58.817	0.358	

at% - atomic percentage

r_{conc} – the ratio of the dopant concentration in respect to the content of the element which it substitutes (Nd, Er substitutes Y sites, Cr substitutes Al sites)

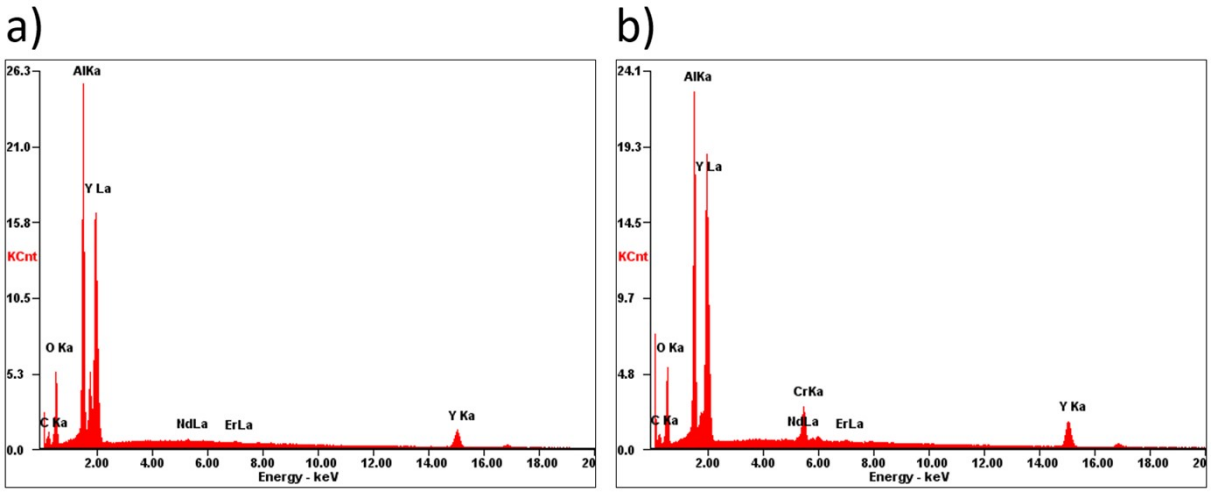

Figure S2. The representative EDS spectra for YAG:Nd^{3+}, Er^{3+} (a) and YAG:Nd^{3+}, Er^{3+}, 10% $Cr^{3+/4+}$ (b).

Table S3. Atomic concentration from the analyzed samples by XPS method.

	The concentration of elements for the YAG:1% Nd^{3+}, 1% Er^{3+}, x% $Cr^{3+/4+}$ samples (%):			
Element	x = 1%	x = 5%	x = 10%	x = 20%
Al	11.74	12.97	10.4	7.25
Y	6.73	8.21	6.9	4.6
C	40.25	32.23	43.28	50
O	36.58	42.24	35.07	34.1
N	4.54	4.17	3.96	3.48
Cr	0	0.17	0.39	0.56

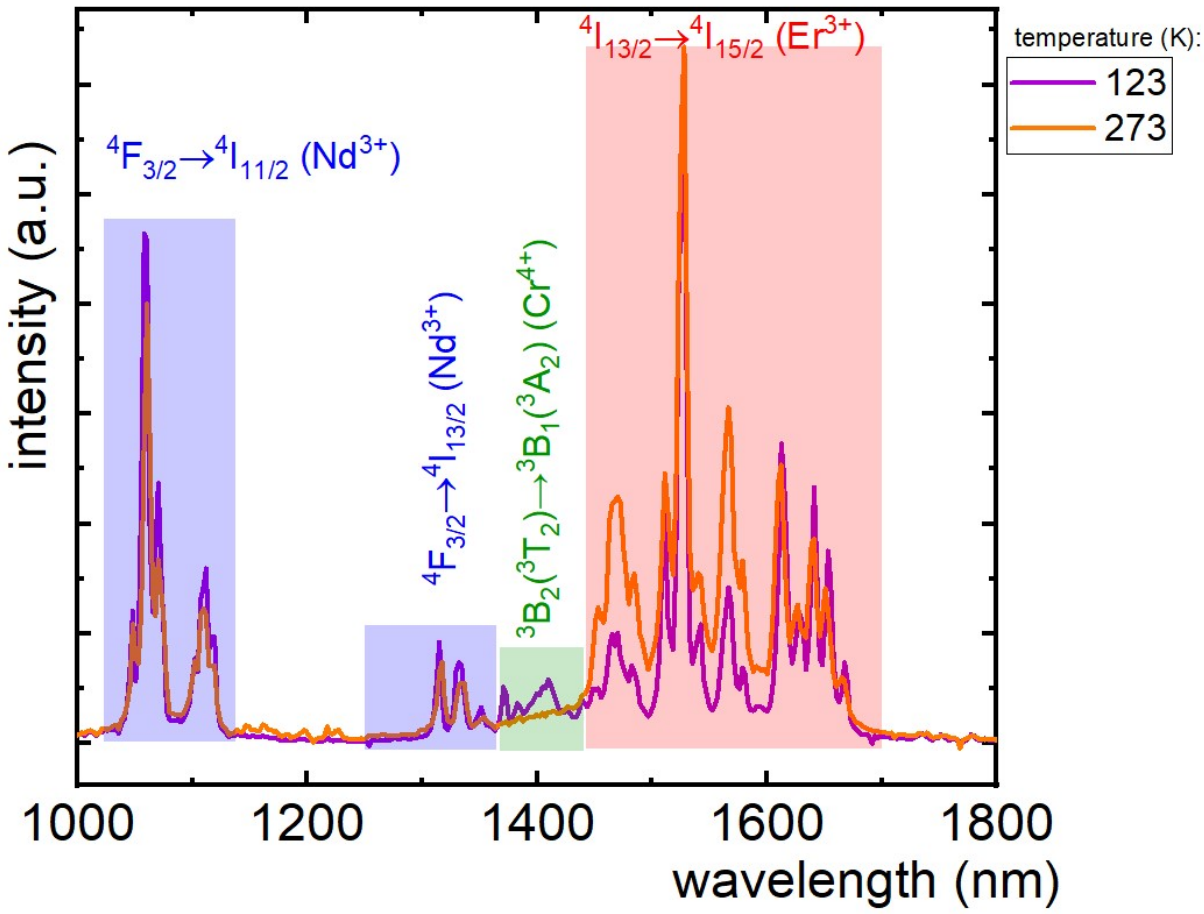

Figure S3. The emission spectra of YAG:1% Nd^{3+}, 1% Er^{3+}, 5% $Cr^{3+/4+}$ at 123 K and at 273K .

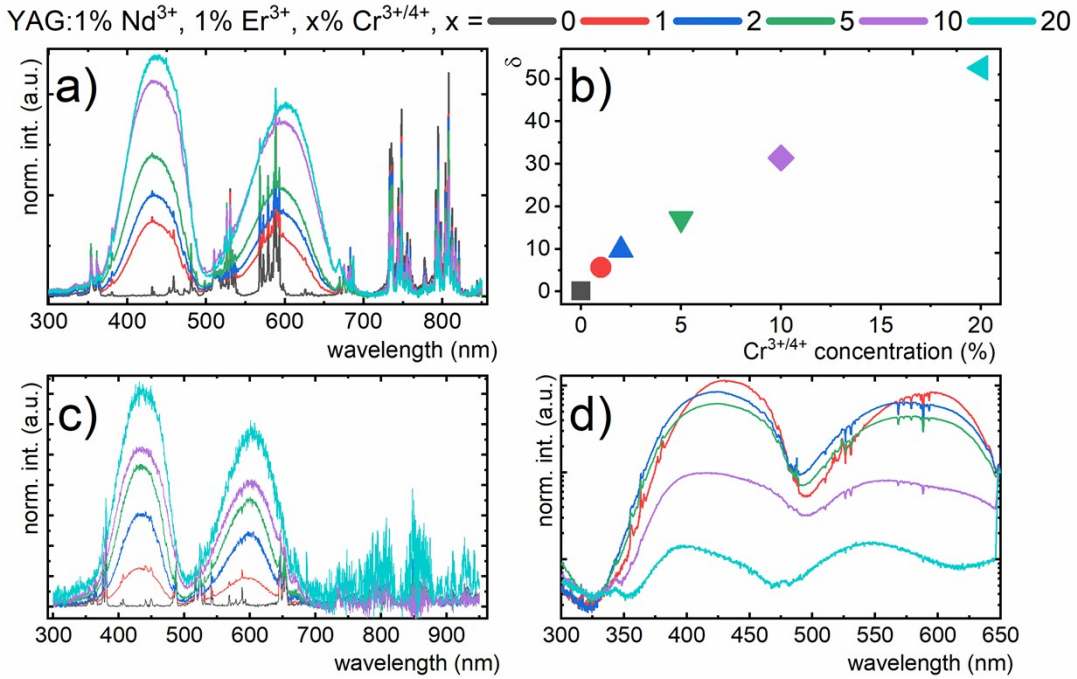

Figure S4. The influence of $Cr^{3+/4+}$ ions concentration on excitation spectra in YAG:1% Nd^{3+}, 1% Er^{3+}, x% $Cr^{3+/4+}$ for 1064 nm (a) and on the contribution parameter δ (b), for 1530 nm (c) and for 445 nm (d).

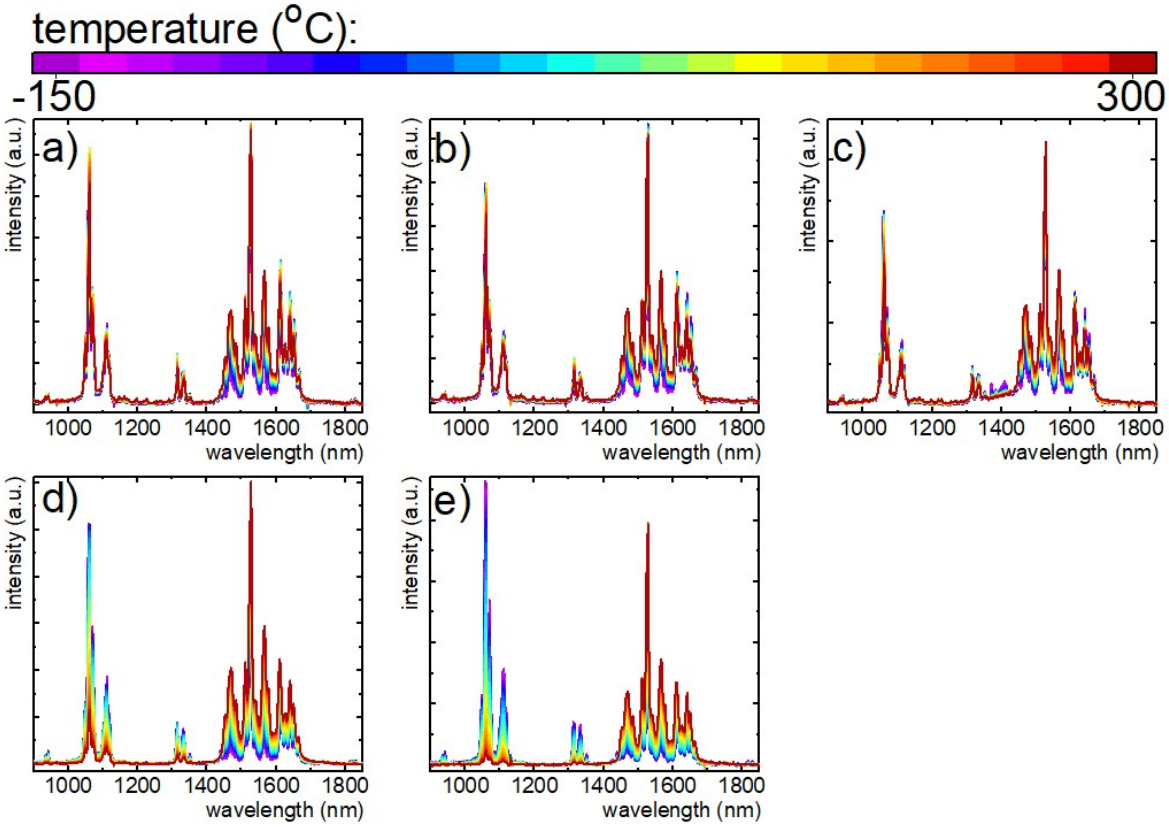

Figure S5. The thermal evolution of the NIR range of emission spectra of YAG:1% Nd^{3+}, 1% Er^{3+}, x% $Cr^{3+/4+}$ powders with λ_{exc} = 445 nm, where x = 1 (a), 2 (b), 5 (c), 10 (d), 20 (e).

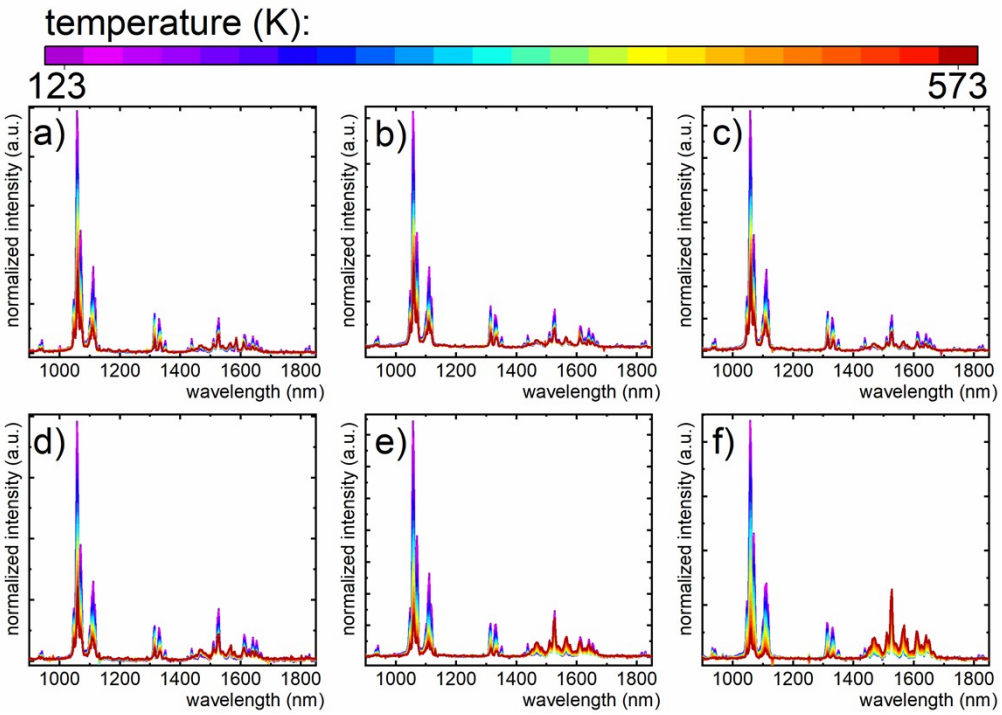

Figure S6. The thermal evolution of emission spectra of YAG:1% Nd^{3+}, 1% Er^{3+}, x% $Cr^{3+/4+}$ powders with λ_{exc} = 793 nm, where x = 0 (a), 1 (b), 2 (c), 5 (d), 10 (e), 20 (f).

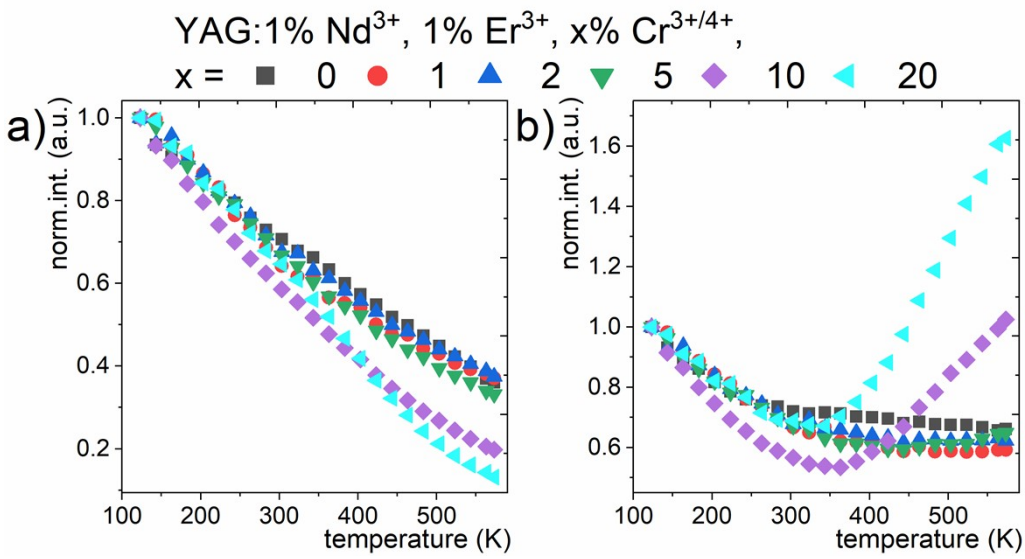

Figure S7. The thermal evolution of integral band intensities of $^4F_{3/2} \rightarrow {}^4I_{11/2}$ transition of Nd^{3+} ion (a) and $^4I_{13/2} \rightarrow {}^4I_{15/2}$ electronic transition of Er^{3+} ion (b) excited by λ_{exc} = 793 nm.

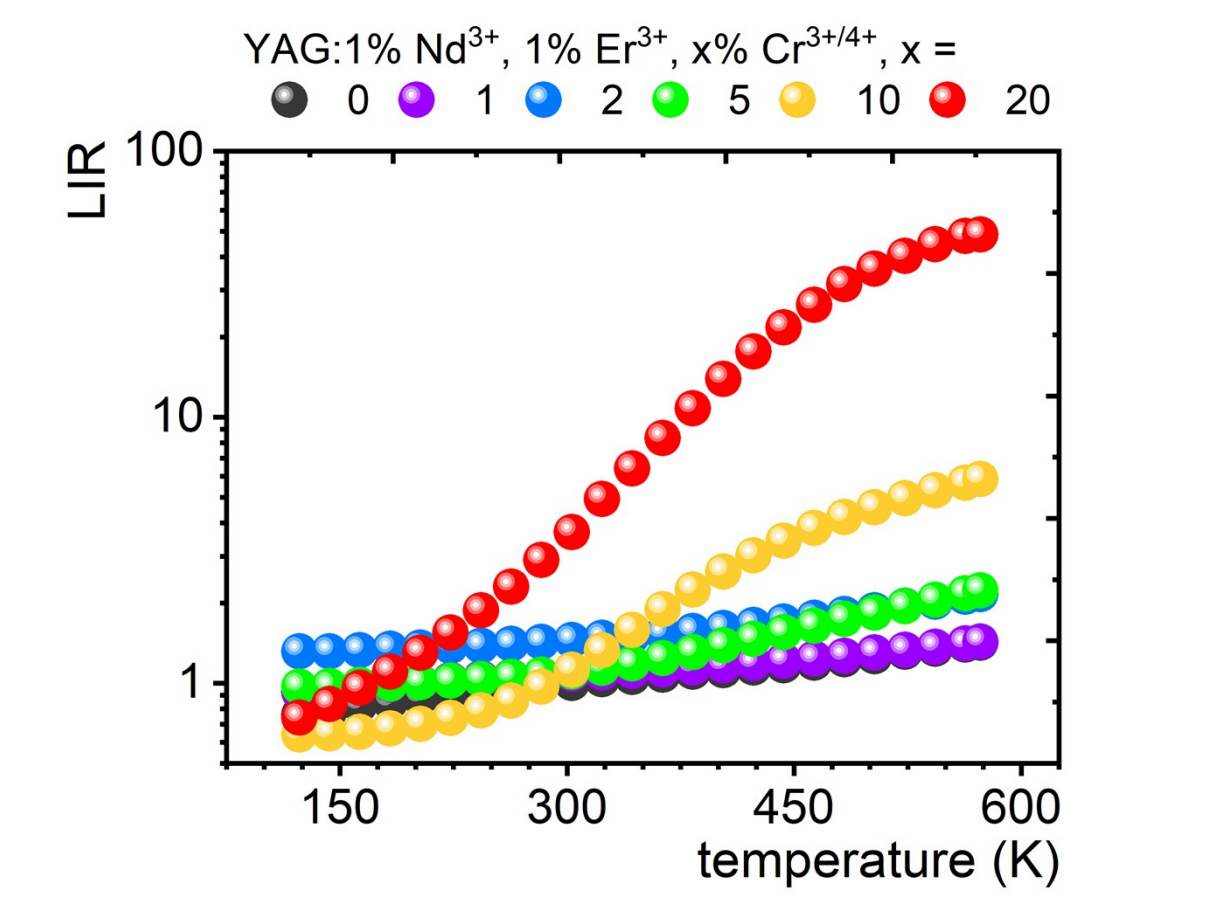

Figure S8. Thermal dependence of LIR calculated on the unnormalized data for different Cr3+/Cr4+ dopant concentration

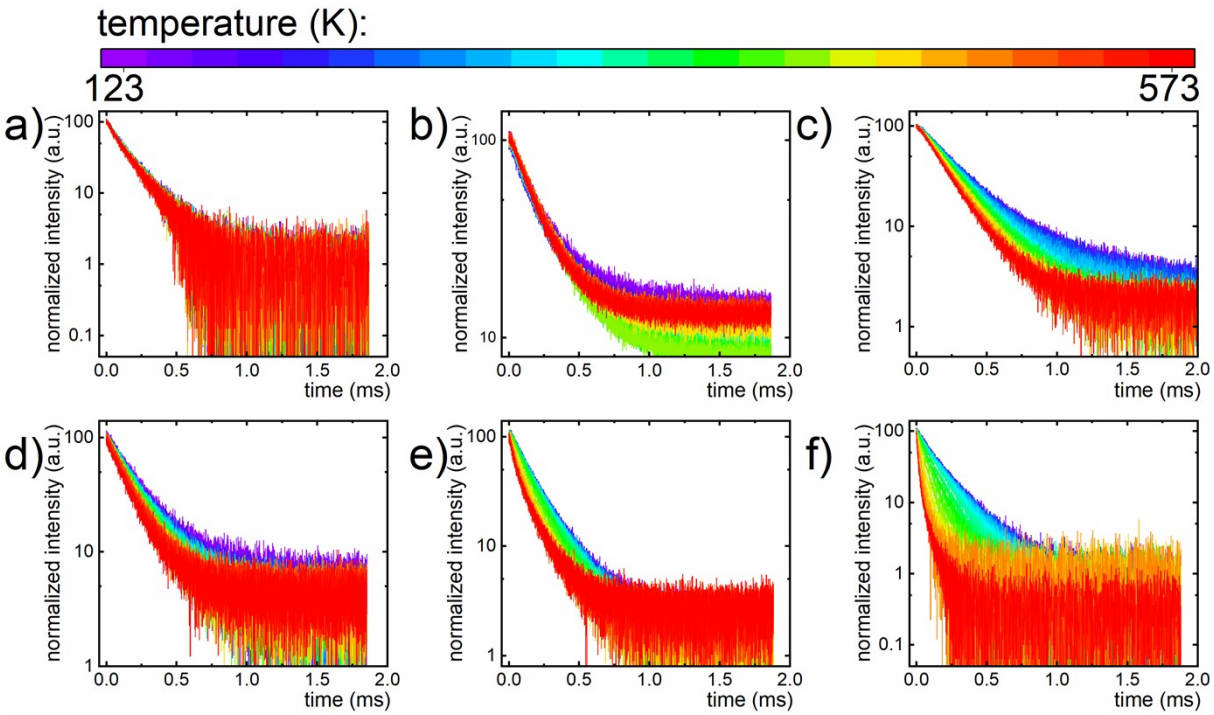

Figure S9. The thermal evolution of luminescent decays in YAG:1% Nd^{3+}, 1% Er^{3+}, x% $Cr^{3+/4+}$ for 1064 nm (Nd^{3+} excited state), where x = 0 (a), 1 (b), 2 (c), 5 (d), 10 (e), 20 (f).

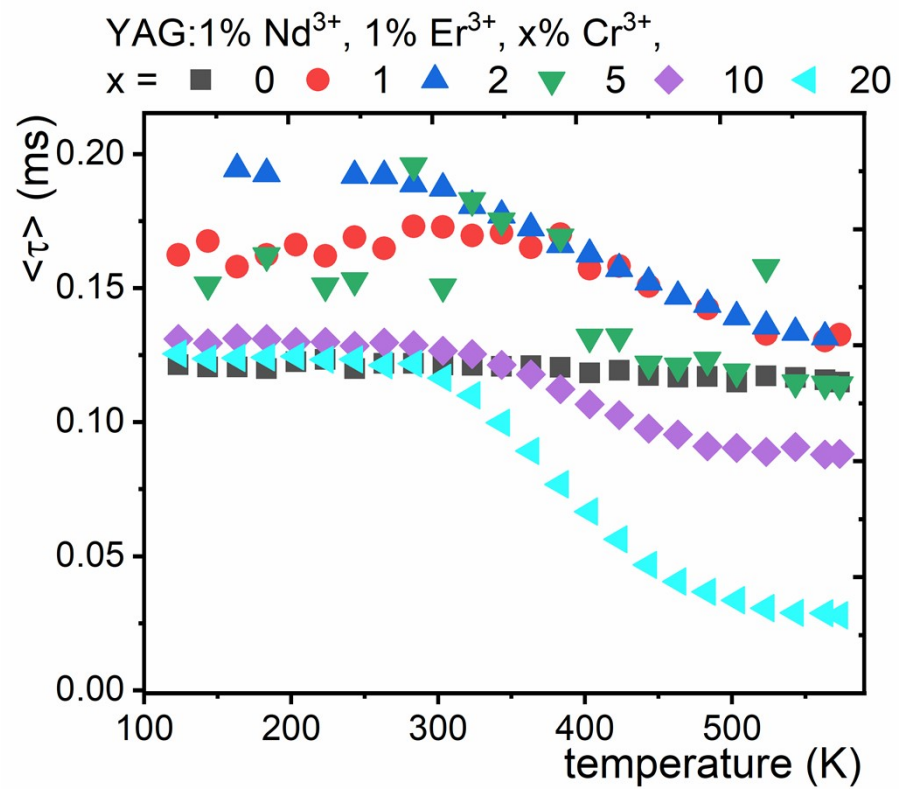

Figure S10. The thermal evolution of average lifetime of Nd^{3+} excited state for YAG:1% Nd^{3+}, 1% Er^{3+}, x% $Cr^{3+/4+}$ powders.

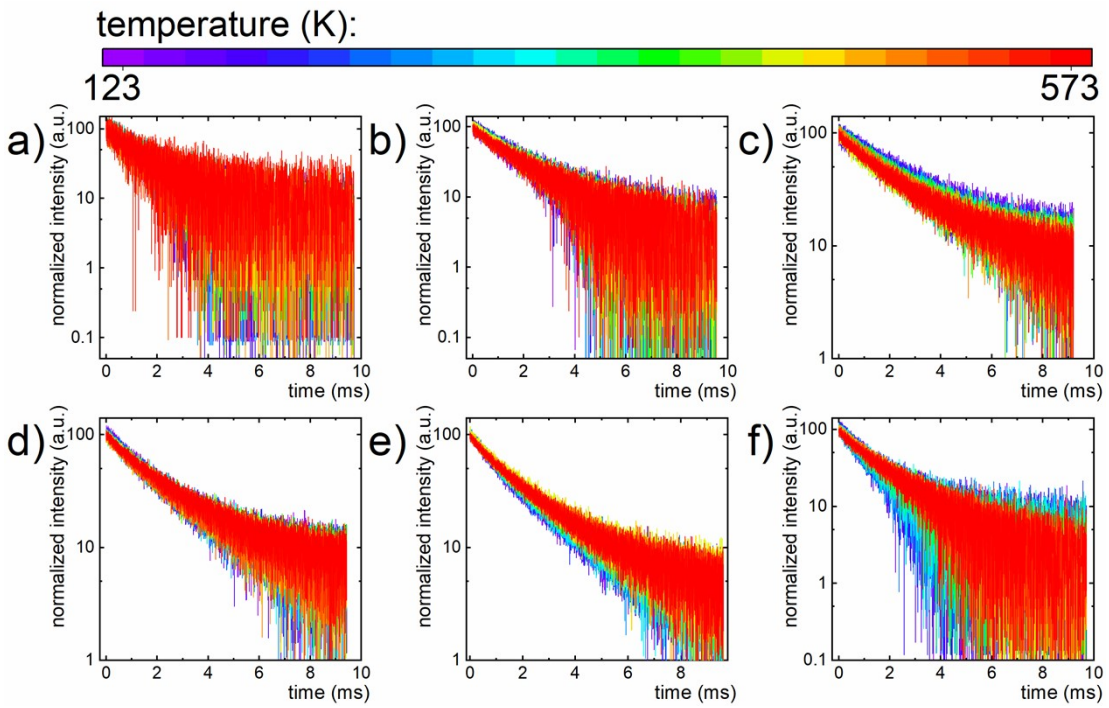

Figure S11. The thermal evolution of luminescent decays in YAG:1% Nd^{3+}, 1% Er^{3+}, x% $Cr^{3+/4+}$ for 1530 nm (Er^{3+} excited state), where x = 0 (a), 1 (b), 2 (c), 5 (d), 10 (e), 20 (f).

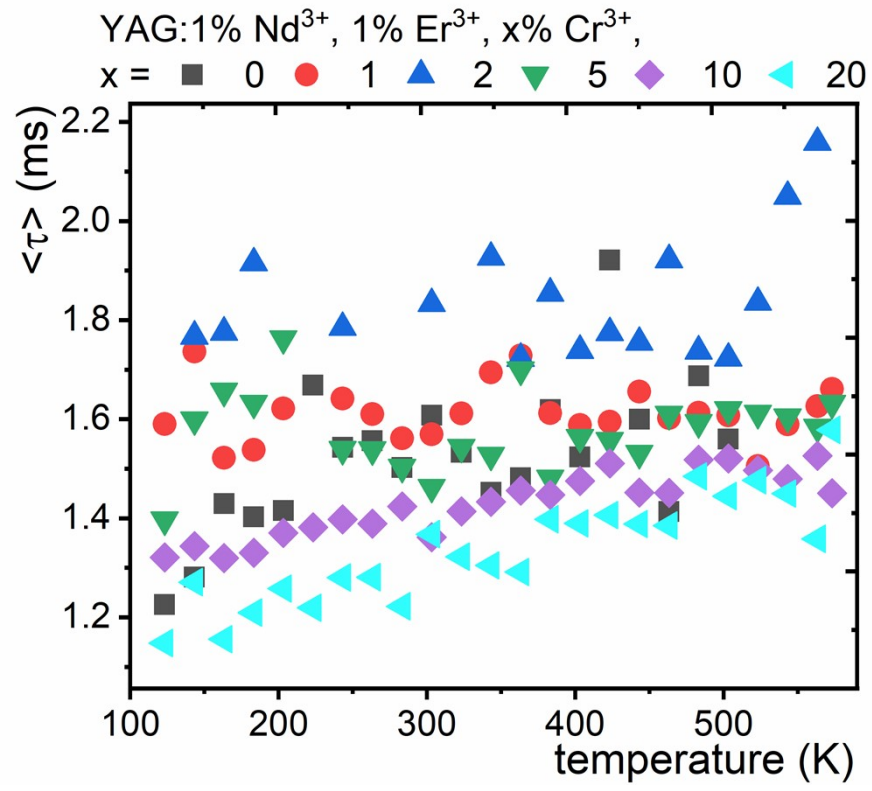

Figure S12. The thermal evolution of average lifetime of Er^{3+} excited state for YAG:1% Nd^{3+}, 1% Er^{3+}, x% $Cr^{3+/4+}$ powders.

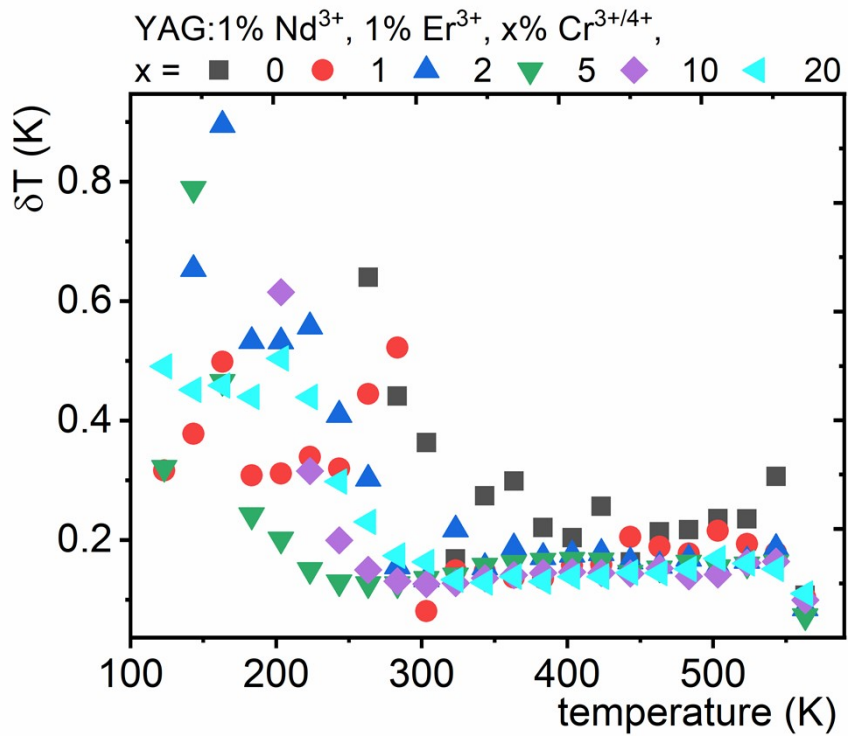

Figure S13. The thermal dependence of temperature estimation uncertainty for different $Cr^{3+/4+}$ concentration in the YAG:1% Nd^{3+}, 1% Er^{3+}, x% $Cr^{3+/4+}$.

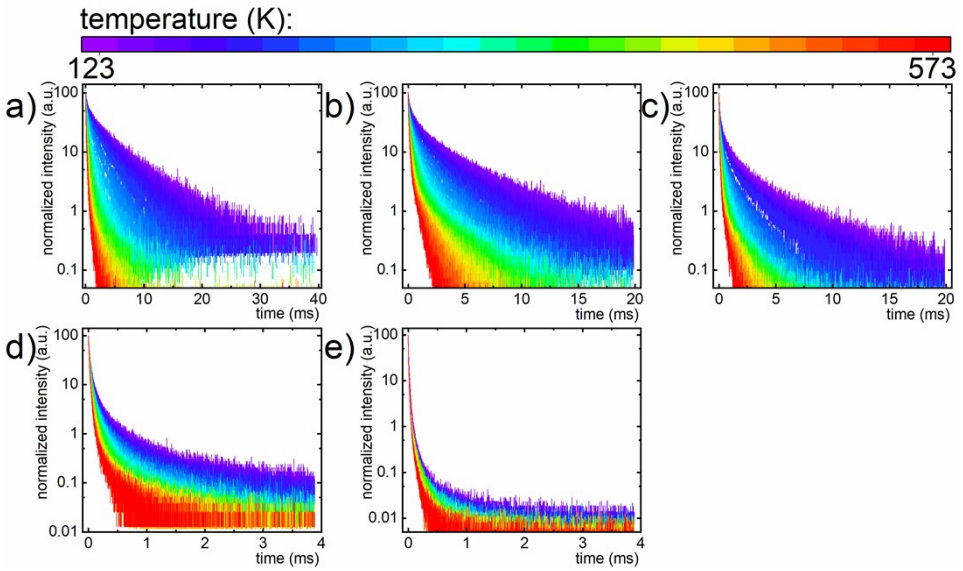

Figure S14. The thermal evolution of luminescent decays in YAG:1% Nd^{3+}, 1% Er^{3+}, x% $Cr^{3+/4+}$ for 445 nm (Cr^{3+} excited state), where x = 1 (a), 2 (b), 5 (c), 10 (d), 20 (e).

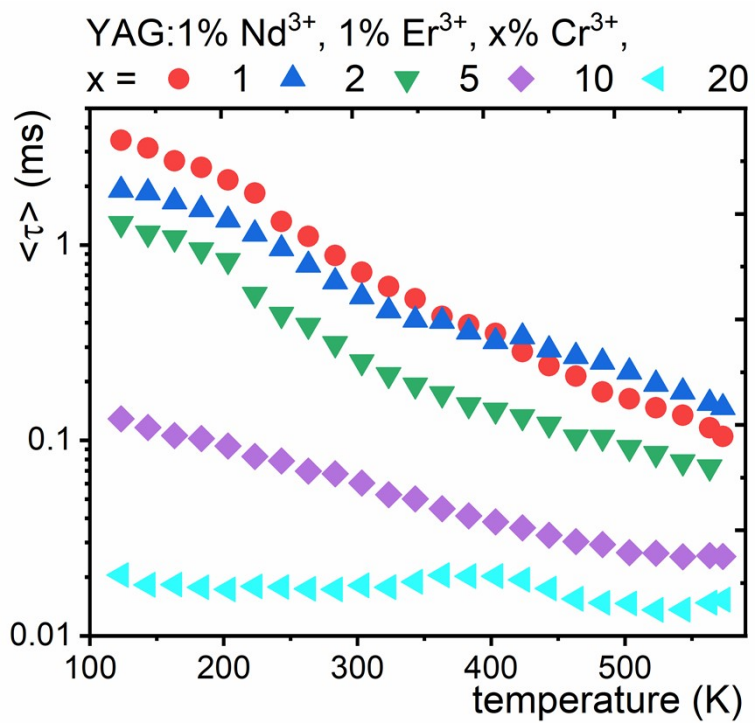

Figure S15. The thermal evolution of average lifetime of Cr^{3+} excited state for YAG:1% Nd^{3+}, 1% Er^{3+}, x% $Cr^{3+/4+}$ powders.